A&A 490, L19–L22 (2008)
DOI: 10.1051/0004-6361:200810926

Astronomy & Astrophysics

Letter to the Editor

Methane clathrate hydrate FTIR spectrum

Implications for its cometary and planetary detection

E. Dartois⋆ and D. Deboffle

Institut d'Astrophysique Spatiale, UMR-8617, Université Paris-Sud, Bât. 121, 91405 Orsay, France
e-mail: emmanuel.dartois@ias.u-psud.fr

Received 6 September 2008 / Accepted 16 September 2008

ABSTRACT

Context. The physical behaviour of methane clathrate hydrate, a crystallographic ice crystal is of major importance for both the earth and the stability of gases in many astrophysical bodies (planets, comets, etc.).
Aims. We provide an infrared spectroscopic identification for astrophysical methane clathrate hydrates and investigate the crystal field experienced by the trapped molecule.
Methods. A methane clathrate crystal was produced in a moderate-pressure optical cell. Using FTIR spectroscopy, the ν_3 asymmetric CH-stretching mode of the entrapped methane molecule is recorded from 7 K to 80 K, then back to 7 K.
Results. It is shown that the trapped methane molecules in the clathrate hydrate is a quasi rotor, displaying gaseous behaviour at low temperatures. A series of ro-vibrational specific lines is observed, shifted in frequency by the water-ice cage interactions with the trapped methane molecules. Because these transitions are unique to methane clathrate hydrate, they represent a crucial identification pattern for astrophysical icy bodies at low temperatures, such as comets and/or interstellar grains.

Key words. molecular data – solar system: formation – ISM: lines and bands – line: identification – line: profiles

1. Introduction

Clathrate hydrates are inclusion compounds in which a host molecule is trapped in a water-ice crystal. Among the hydrate classes, methane clathrate hydrate plays a preponderant role because of its widespread impact on many fields of science and industry. Present in the permafrost, it may represent a huge energetic resource, more abundant (~10 000 gigatons) than all other fossil fuels combined, according to the U.S. Geological Survey (e.g. Kvenvolden & Lorenson 2001). If controlled, clathrate hydrate could efficiently help in solving storage issues for light hydrocarbons or hydrogen. Methane, the simplest hydrocarbon molecule, is found everywhere in astrophysics, from giant planets' atmospheres (Hammel et al. 2007; Kim et al. 2006; Tran et al. 2006), in their moons, to outer bodies (Brown et al. 2007; Douté et al. 1999), and it sublimates from comets entering the inner solar system. It is also observed as a component of the ice mantles covering interstellar grains in dark clouds (e.g. Oberg et al. 2008, and references therein). In solar system bodies, its observed abundance must be supported either by a chemistry replenishing the environment to compensate for the various methane-destruction mechanisms (photo-dissociation by the sun in planetary upper atmospheres, e.g. Atreya et al. 2006, chemical reactions). Alternatively, these objects may possess a reservoir preserving the sublimation of gases out of their pure substance equilibrium vapour pressures (e.g. Mousis & Schmitt 2008; Bar-Nun et al. 2007); therefore, the study of methane hydrates, in general, and clathrate hydrates, in particular, represent key issues both for their observability and their ability to constrain chemical balance.

Clathrate hydrates pertain to the few crystals hosting possibly rotating molecules. The interaction of the entrapped molecule with the ice can also give insight into the field experienced inside the crystal. The clathrate hydrates behaviour has therefore been investigated, among other techniques, by Raman (e.g. Sum et al. 1997) and (far-)infrared (Richardson et al. 1985; Klug & Whalley 1973; Bertie & Jacobs 1982; Fleyfel & Devlin 1988) spectroscopies, as well as neutron scattering (Gutt et al. 2002; Prager & Press 2006) and RMN techniques (Kleinberg et al. 2003; Nakayama et al. 2003; Davidson et al. 1977). Pure methane hydrate forms cubic structure I, with two small water-molecule pentagonal dodecahedron cages ($S = 5^{12}$) and six large hexagonal truncated trapezohedron cages ($L = 5^{12}6^2$) in the unit cell, with the general formula ($2S.6L.46H_2O$). At liquid-helium cryogenic temperatures, the methane ground-state rotation inside the cages has been shown with the neutron diffraction techniques above to behave like an almost free rotor with a modified moment of inertia, attributed to longer C-H length in the trapped state.

In this Letter we present the infrared vibrational spectrum of the methane clathrate at low temperatures for the ν_3 triply degenerate asymmetric stretching mode. The experiments are first described in Sect. 2 and the results in Sect. 3. We discuss the implications for astrophysics in Sect. 4 and conclude in Sect. 5.

2. Experiments

A dedicated evacuable enclosed cell was built to study the low-temperature methane clathrate hydrate infrared spectrum. The cell in copper was attached and thermally coupled to a liquid

⋆ Part of the equipment used in this work has been financed by the French INSU-CNRS program the "Physique et Chimie du Milieu Interstellaire" (PCMI).

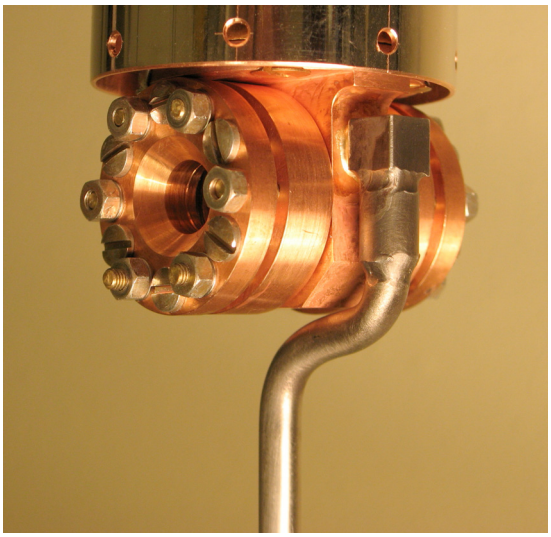

Fig. 1. Low-temperature, moderate-pressure closed cell used to nucleate and characterise the methane clathrate hydrate. The top is attached to a liquid He transfer cold finger, masked by a thermal shield cylinder. The lower injection tube is used both to inject gaseous water and methane, as well as to evacuate it once the hydrate is formed. The two cylindrical copper parts support the MgF_2 windows, offering a 5 mm radius aperture to the infrared beam.

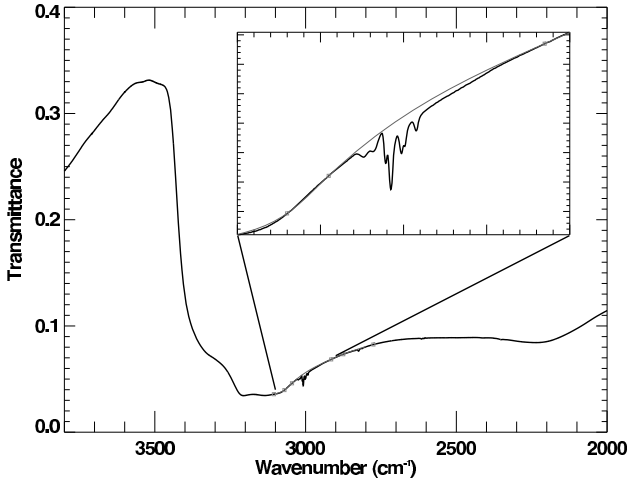

Fig. 2. Stretching-mode FTIR spectrum of the methane clathrate hydrate as recorded at 7 K. The transmittance is dominated by the large water-ice OH stretching modes absorption band, deformed by scattering probably due to the growth of grainy textured hydrate ice grains. The methane infrared active stretching modes appear in the long wavelength wing of the ice feature. A close-up is shown for clarity, together with the adopted local continuum used to extract methane the absorption contribution.

He-transfer cold finger, placed in an high-vacuum, evacuated cryostat ($P < 10^{-7}$ mbar). Thick infrared transmitting MgF_2 windows were sealed with indium gaskets to the two lateral ports allowing the spectrometer beam to monitor the clathrate hydrate spectrum. The lower part of the cell possesses a solded stainless steel injection tube for the entrance of gas or its evacuation. A schematic view of the cell is shown in Fig. 1.

The formation of the methane hydrate follows a procedure that satisfies both its nucleation and prevents the sample from becoming optically thick to the infrared beam. Water vapour is first injected into the evacuated cell maintained at a temperature just above the water's triple point. Because of the gradual increase of pressure in the cell during injection, liquid water condenses out on the MgF_2 windows, and methane gas is injected immediately after at moderate pressures (40 bars). The cell is then cooled to 255 K as rapidly as possible to form a hexagonal ice film as monitored by the profile change of the high-wavenumber side of the ice OH-stretching mode not hidden in the spectrum by gaseous CH_4 absorptions. The cell is maintained in this state, more than 20 bars above the clathrate hydrate stability line at this temperature, typically during two days. The methane diffuses into the thin ice film present on the two MgF_2 interfaces, kept under pressure, allowing the hydrate nucleation from the solid phase. In a next step, the cell temperature is then lowered using liquid He. The lowest temperature reached (7 K) is driven by the thermal escape through the long injection tube connected to room temperature at the other side and exposed cell parts. The gaseous methane is progressively evacuated from the cell. At this stage, care is taken to follow a path in the P-T methane phase diagram close to, but just below, the vaporisation ($T \gtrsim 90$ K) and sublimation ($T \lesssim 90$ K) curves to stay above the expected clathrate hydrate dissociation curve. In these experiments, the successful formation of methane clathrate hydrate can only be checked at this stage, when all the CH_4 gas has been evacuated while maintaining the 7 K temperature. The FTIR spectra are recorded in the 7 K to 80 K range with a Bruker IFS 66v at a resolution of 0.5 cm^{-1}, with a globar IR source, KBr beamsplitter, and an HgCdTe detector cooled at LN_2. The excursion to record the spectrum at 80 K was short enough (~15 min) to prevent an eventual and progressive clathrate hydrate dissociation observed on rather short time scales in the previous experiments at higher temperatures.

The raw methane clathrate hydrate spectra as recorded at 7 K is shown in Fig. 2. It is dominated by broad water-ice vibrational transitions, the thin lines superimposed on the water-ice features pertaining to encaged methane related transitions. Due to the necessity of maximising the optical depth and thus condense sufficient water on the MgF_2 windows, the ice deposit is grainy and additional non uniformity during clathrate growth induces some scattering, giving rise to the deformed ice profile observed.

3. Results

3.1. Methane clathrate hydrate CH stretching mode

The clathrate CH_4 ν_3 stretching-mode region of the spectrum is displayed in Figs. 2 and 3, recorded at cell temperatures of 7, 20, 30, 50, and 80 K to follow the evolution of the line profiles with temperature. A local-continuum smooth spline baseline (shown in the inset of Fig. 2) was removed to account for the strong hydrate OH stretching mode wing. An observed series of ro-vibrational lines is attributed to the methane branches, shifted downward in frequency with respect to gaseous methane. A synthetic gas-phase model using the line parameter of the HITRAN database (Rothman et al. 2005) was calculated at 7 K, convoluted by a Gaussian profile with approximately the same line width as measured for the clathrate hydrate, to show both the shift and the expected ro-vibrational gas-phase spectrum. An ice film spectrum of pure CH_4 recorded at 10 K is also shown for comparison (Hudgins et al. 1993). At this temperature, the CH_4 cubic phase displays some substructure assignable to the hindered rotation of some methane molecules in the ice (e.g. Chapados & Cabana 1972; Kobashi et al. 1977), but apart from $^{13}CH_4$ ν_3 contributions, methane in cubic phase II do not display strong transitions shortward of 3000 cm^{-1}. In addition, no sharp transition to the

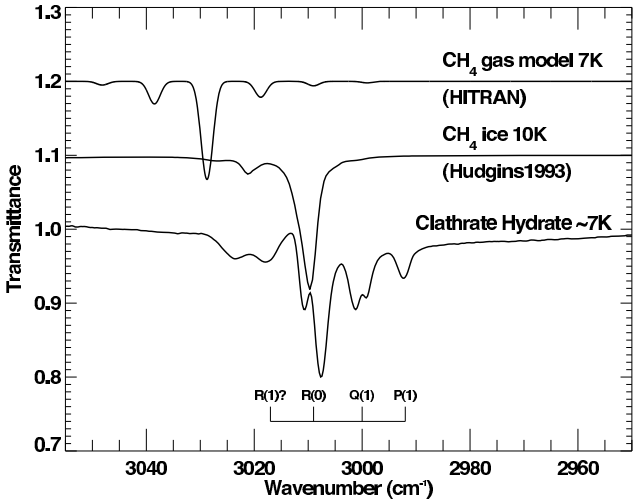

Fig. 3. Stretching-mode FTIR spectrum of the methane clathrate hydrate as recorded at 7 K. A comparison with thin-film methane ice at 10 K (Hudgins et al. 1993) and gaseous methane model shows the almost free state of the methane molecules and the wavenumber shift induced by the cage's force field.

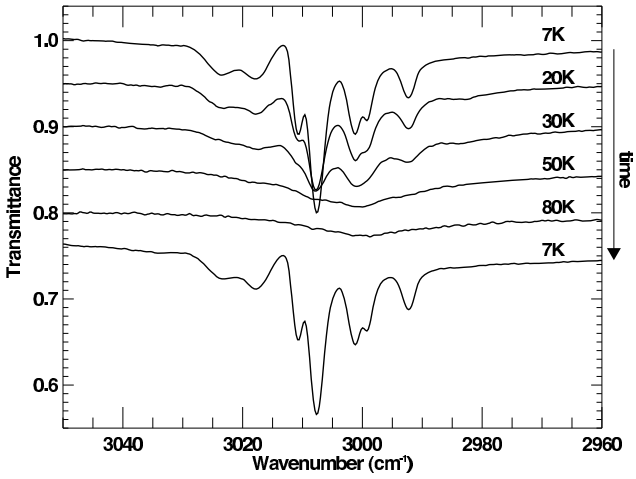

Fig. 4. Temperature evolution of the ν_3 CH stretching mode of methane clathrate hydrate from 7 to 80 K. After a short time excursion to 80 K to avoid the clathrate dissociation, the cell is cooled again to 7 K, recovering the initial ro-vibrational pattern.

phase I disordered methane ice expected at 20.4 K is observed, ruling out methane-ice contamination to the spectrum.

The observed individual lines can be ascribed to the ability of the methane molecule to rotate in the clathrate hydrate cages formed, and drives the assignment to methane transitions for molecules trapped in the cages. The influence of the cage shifts the ro-vibrational strongest transitions to lower frequencies by $\Delta\nu \sim 15{-}20\ \mathrm{cm}^{-1}$. In addition, the lines display substructures that trace the lift of degeneracy imposed by the crystal field sharing similarities with methane trapped in para-H_2 solids (Tam et al. 1999). The crystal field that induces splitting of the ro-vibrational lines is most clearly observed for the strongest lines. A similar pattern has been explained for methane in the hexagonal compact para-hydrogen crystal (Momose et al. 2004), although the interaction with the para-H_2 matrix is weaker because both the shift and the line width are less pronounced. The D_{6d} clathrate hydrate large-cage symmetry is different from the D_{3h} one for the para-H_2 crystal, but the lift of degeneracy seems to induce a similar pattern. The broader individual lines, however, may not allow all the transition's substructure to be resolved. This would be highly desirable and especially important to identify the small cage transitions after removal of the large-cage ones.

Considering the similar cage occupancies expected at the formation temperature (255 K, Sizov & Piotrovskaya 2007; Sloan 1998) and the 6:2 ratio of large-to-small cages in clathrate hydrate of type I, we attribute the deepest transition to the hydrate large cages. The main rotational branches in the large cage are tentatively assigned in Fig. 3 where they reveal the possible presence of additional transitions in the higher wavenumber part of the spectrum (around 3018 and 3025 cm^{-1}), which we believe partly pertains to the second (small-)cage enclathration of methane molecules. The measured Raman active symmetric ν_1 CH stretching mode vibration, associated to methane in the clathrate hydrate large cages, also shifts with respect to the gas phase (~12 cm^{-1}, Sum et al. 1997). This amplitude is slightly lower than the one measured here for the large cages (~15–20 cm^{-1}). If the methane molecules trapped in small cages follow the same trend as in Raman spectra, their infrared transitions should effectively appear a few wavenumbers downward from the gas phase one.

The observed rotational spacing between the observed transitions in large cages (~9 cm^{-1} as compared to about 9.93 cm^{-1} for the gas phase) is close to the one observed for neutron scattering experiments (Gutt 2002; Prager 2006) monitoring ground-state rotational transitions of methane hydrate at low temperatures. The line widths for the transitions are also characteristic.

3.2. Temperature dependence

The temperature evolution of the methane features from 10 K to 80 K shows a progressive broadening of the line width of the individual lines seen at low temperature, which seems to fuse into broad bands. The temperature dependence of the observed spectra does follow the ground-state rotational behaviour observed (Tse 1997); i.e., a damping in the rotation as the temperature is progressively increased above about 30 K. This behaviour is explained by the strong coupling of the trapped methane with lattice modes (Tse 1997) hindering the rotation observed at 7 K.

4. Discussion

Estimates of the presence of clathrate hydrates in astrophysical objects have up to now been largely based on models that essentially implement phase diagrams (e.g. Hersant et al. 2008; Mousis et al. 2008; Prieto-Ballesteros et al. 2005; Kargel & Lunine 1998), sometimes extrapolated at low temperatures. In these astrophysical environnements where clathrate hydrates are possibly stable against dissociation, questioning their formation and associated kinetics should readily supersede stability curves determinations. The conditions for clathrate hydrates formation at rather high temperatures may easily be encountered on some planetary surfaces. Alternatively, at much lower temperatures, in a micro-grainy textured water ice offering a huge open surface-to-volume ratio, the building of hydrate cages may proceed by adsorption/reconstruction of the ice surface, and the mixing rate or renewing of the ice surface strongly influences the formation kinetics.

Direct diffusion of methane at cometary and interstellar grain temperatures into an ice Ih is probably unlikely because of the very low diffusivity of methane (and other gases) at temperatures

below 100 K. Using the methane diffusion coefficient into the ice estimated experimentally by Takeya et al. (2002), corresponding to a diffusion activation energy of 20.1 kJ/mol, the mean time for a diffusion length of only one micron exceeds 1 Gy at temperatures below about 50 K, thereby impeding efficient formation by diffusion at such low temperatures. In addition to the low-temperature, diffusion-limited growth of the clathrate hydrate, even at higher temperatures, once a crust of clathrate hydrate is formed it will add an activation barrier. The outside methane molecule will have to overcome this barrier for the propagation of the methane into the bulk of the ice to proceed (e.g. Wang et al. 2002).

The methane clathrate hydrate FTIR spectrum at the low temperature presented in this Letter clearly shows CH-stretching, ro-vibrational transitions of a quasi-free rotating molecule, thus spectroscopically distinct from the other methane forms, like the phase II cubic at $T \leq 20.4$ K, the phase I above (e.g. Trotta 1996), or embedded as a simple hydrate. The confirmation of its (non-ambiguous) detection can probably only be secured by spectroscopic means. This is what is done in the laboratory using e.g. Raman or neutron-scattering spectroscopies, two techniques unfortunately not easily carried over to astrophysical observations or space probes. By contrast, infrared spectroscopy is a major remote means of identifying and distinguishing between a clathrate hydrate crystal and another chemical-ice mixture displaying a roughly similar thermodynamic behaviour. One should be able to record the fingerprints in the infrared spectrum by observing both the ro-vibrational line progression at a low temperature and the capability of the two distinct cages both containing methane to give rise to a characteristic profile.

The observation of methane hydrate ro-vibrational transitions at low temperatures or of the cages field induced shift at higher temperatures constitutes necessary steps in its astrophysical identification. A remote observation of clathrate hydrates in the high-temperature planetary surfaces will be performed best using enclathrated methane overtone and combination modes because the ν_3 mode will be saturated. As their surfaces are above 30 K, the rotational substructure observed at a low temperature will merge into broad bands, but the field experienced by the methane molecule induces a shift in band position that will make the spectrum different from the other methane phases. Outer bodies, such as TNOs and comets before entering the inner solar system, do possess lower surface temperatures that are low enough to be able to see the rotational substructures, but again combination modes will be more appropriate for reflectance measurements. Despite considerable efforts, the remote observations of cometary ices are still in their early days, and the Hale-Bopp observations (Lellouch et al. 1998) and the Deep impact Tempel 1 observations do not show any methane absorptions (e.g. Sunshine et al. 2007). Some models require enclathrated methane to explain its late degassing behaviour, so more observational efforts must be made in that direction on the basis of our new spectra. The CH_4 molecule is observed in interstellar medium ice mantles mainly through another mode (ν_4 around 1300 cm^{-1}), displaying a broad and structureless line profile that points to the absence of clathrate hydrates, as one would expect for a methane rotor substructure in this mode, too, and it is thus explained well with simple methane hydrates. The only clear detection of the ν_3 mode by Boogert et al. (2004) displays neither the right position nor any rovibrational spectrum, also pointing to the absence of methane clathrate hydrate.

To better control the hydrate film nucleation, to access weaker infrared active transitions (combinations and overtones), and to span a wider wavenumber range, an improved cell is being tailored. These developments will not only help toward understanding the observable spectroscopic behaviour but will also aim at studying methane clathrate formation kinetics at a low temperature.

Acknowledgements. We wish to acknowledge fruitful discussions and/or technical support from D. Barbet, M. Bouzit, M. Chaigneau, A. Chardin, N. Coron, B. Crane, C. Dumesnil, J.-J. Fourmond, T. Redon, G. Renoux.

References

Atreya, S. K., Adams, E. Y., Niemann, H. B., et al. 2006, Planet. Space Sci., 54, 1177
Bar-Nun, A., Notesco, G., & Owen, T. 2007, Icarus, 190, 655
Bertie, J. E., & Jacobs, S. M. 1978, J. Chem. Phys., 69, 4105
Bertie, J. E., & Jacobs, S. M. 1982, J. Chem. Phys., 77, 3230
Boogert, A. C. A., Blake, G. A., & Öberg, K. 2004, ApJ, 615, 344
Brown, M. E., Barkume, K. M., Blake, G. A., et al. 2007, AJ, 133, 284
Chapados, C., & Cabana, A. 1972, Can. J. Chem., 50, 3521
Davidson, D. W., Garg, S. K., Gough, S. R., Hawkins, R. E., & Ripmeester, J. A. 1977, Can. J. Chem., 55(20), 3641
Douté, S., Schmitt, B., Quirico, E., et al. 1999, Icarus, 142, 421
Fleyfel, F., & Devlin, J. P. 1988, J. Phys. Chem., 92, 631
Gutt, C., Press, W., Huller, A., & Tse, J. S. 2002, Appl. Phys. A, 74, 1299
Hammel, H. B., Sitko, M. L., Lynch, D. K., et al. 2007, AJ, 134, 637
Hersant, F., Gautier, D., Tobie, G., & Lunine, J. I. 2008, Planet. Space Sci., 56, 1103
Hudgins, D. M., Sandford, S. A., Allamandola, L. J., & Tielens, A. G. G. M. 1993, ApJS, 86, 713
Kargel, J. S., & Lunine, J. I. 1998, Sol. System Ices, 227, 97
Kim, J. H., Kim, S. J., Geballe, T. R., Kim, S. S., & Brown, L. R. 2006, Icarus, 185, 476
Kleinberg, R. L., Flaum, C., Griffin, D. D., et al. 2003, J. Geophys. Res., 108(B10), 2508
Klug, D. D., & Whalley, E. 1973, Can. J. Chem., 51(24), 4062
Kobashi, K., Okada, K., & Yamamoto, T. 1977, J. Chem. Phys., 66, 5568
Kvenvolden, K. A., & Lorenson, T. D. 2001, A Global Inventory of Natural Gas Hydrate Occurrence, Geophysical monograph (Washington, DC, USA: American Geophysical Union editors), 124, 3
Lellouch, E., Crovisier, J., Lim, T., et al. 1998, A&A, 339, L9
Momose, T., Hoshina, H., Fushitani, M., & Katsuki, H. 2004, Vib. Spectroscopy, 34(1), 95
Mousis, O., & Schmitt, B. 2008, ApJ, 677, L67
Mousis, O., Alibert, Y., Hestroffer, D., et al. 2008, MNRAS, 383, 1269
Nakayama, H., Klug, D. D., Ratcliffe, C. I., & Ripmeester, J. A. 2003, Chemistry – A European Journal, 9(13), 2969
Öberg, K. I., Boogert, A. C. A., Pontoppidan, K. M., et al. 2008, ApJ, 678, 1032
Prager, M., & Press, W. 2006, J. Chem. Phys., 125, 214703
Prieto-Ballesteros, O., Kargel, J. S., Fernández-Sampedro, M., et al. 2005, Icarus, 177, 491
Tam, S., Fajardo, M. E., Katsuki, H., et al. 1999, J. Chem. Phys., 111(9), 4191
Takeya, S., Ebinuma, T., Tsutomu, U., Nagao, J., & Hideo, N. 2002, J. Cryst. Growth, 237, 379
Trotta, F. 1996, Ph.D. Thesis
Richardson, H. H., Wooldridge, P. J., & Devlin, J. P. 1985, J. Chem. Phys., 83, 4387
Rothman, L. S., Jacquemart, D., Barbe, A., et al. 2005, J. Quant. Radiat. Spectrosc. Trans., 96, 139
Sizov, V. V., & Piotrovskaya, E. M. 2007, J. Phys. Chem. B, 111, 11, 2886
Sloan, E. D. 1998, Clathrate Hydrates of Natural Gases, 2nd edn. (CRC Press)
Sunshine, J. M., Groussin, O., Schultz, P. H., et al. 2007, Icarus, 191, 73
Sum, A. K., Burruss, R. C., & Sloan, E. D. 1997, J. Phys. Chem. B Mater. Surf. Interfaces Biophys., 101, 7371
Tran, H., Flaud, P.-M., Fouchet, T., Gabard, T., & Hartmann, J.-M. 2006, J. Quant. Radiat. Spectrosc. Trans., 101, 306
Tse, J. S., Ratcliffe, C. I., Powell, B. M., Sears, V. F., & Handa, Y. P. 1997, J. Phys. Chem., 101, 4491
Wang, X., Schultz, A., & Halpern, Y. 2002, J. Phys. Chem. A, 106, 32, 7304